



# IJRASET

International Journal For Research in  
Applied Science and Engineering Technology



# INTERNATIONAL JOURNAL FOR RESEARCH

IN APPLIED SCIENCE & ENGINEERING TECHNOLOGY

**Volume:** 12    **Issue:** 1    **Month of publication:** January 2024

**DOI:** <https://doi.org/10.22214/ijraset.2024.58129>

[www.ijraset.com](http://www.ijraset.com)

Call:  08813907089

E-mail ID: [ijraset@gmail.com](mailto:ijraset@gmail.com)

# Statistical Analysis and Optimization of a Single-Effect Vapor Absorption Refrigeration Cycle

Kapil Jain<sup>1</sup>, Basant Kumar Chourasia<sup>2</sup>

<sup>1,2</sup>Department of Mechanical Engineering, Jabalpur Engineering College, Jabalpur, (M.P.), India

**Abstract:** This study employs Response Surface Methodology (RSM) with a Box-Behnken design to optimize the Coefficient of Performance (COP) in a Single-Effect Vapor Absorption System. The thermodynamic model considers a 1-ton refrigeration (TR) system utilizing Lithium bromide-water as the refrigerant, and simulations are conducted using the Engineering Equation Solver (EES). The optimization process identifies optimal values for the generator, absorber, condenser, and evaporator temperatures, set at 90°C, 33°C, 33°C, and -5°C, respectively, resulting in an achieved optimum COP of 0.716. Statistical analysis through ANOVA of the quadratic regression model reveals a significant F-value of 110.62, with a low probability value ( $p=0.0003$ ), attesting to the model's robustness. Key statistical metrics for the model encompass a standard deviation (Std. Dev.) of 0.0059, a mean of 0.8956, a coefficient of variation (C.V. %) of 0.6559, an  $R^2$  of 0.9901, an adjusted  $R^2$  of 0.9811, a predicted  $R^2$  of 0.9159, and an adequate precision of 38.2967. This research offers crucial insights into enhancing the performance of a Single-Effect Vapor Absorption System, thereby contributing to the advancement of energy-efficient refrigeration technologies.

**Keywords:** Single-effect vapor absorption system, Box-Behnken design, mathematical modelling, optimization, ANOVA, COP.

## I. INTRODUCTION

The depletion of fossil fuels, such as coal, oil, and natural gas, as well as the growing harm these fuels cause, make renewable energy sources more and more necessary. As a result, the adoption of absorption refrigeration systems (ARSs) in lieu of vapor compression refrigeration systems has gained traction in recent years. The following are the main benefits of ARSs: Depending on the working fluid pairs employed in the system, they don't harm the ozone layer and can take advantage of a number of sustainable energy sources such as solar energy (Wang et al. [1]) or geothermal energy (Salhi et al. [2]). Marashli et al. [3] created a model for a solar-powered cooling system using Lithium Bromide-Water. Using MATLAB/Simulink, they found the best operating temperatures to avoid crystallization and investigated improving the heat exchanger solution. The system had a cooling capacity of 120 kW and used 243.3 m<sup>2</sup> evacuated tube solar collectors. The generator's temperature was found to be the critical factor for optimal performance, achieving a COP of 0.74 at 110 °C.

Özakin and Kaya [4] conducted an experimental and thermodynamical analysis to study the effects of mass flow rate, temperature, and material type on the thermal and exergy efficiency of an air-based PVT system. They used Taguchi and ANOVA methods to analyze the data. The study found that fin material, airflow rate, and panel temperature were the most effective control parameters on both thermal and exergy efficiencies. The researchers also determined the optimum combinations of control parameters for both frequent and sparse configurations of all fin materials. Based on the ANOVA results, fin material had a very dominant effect on both thermal and exergy efficiency, while fan speed had a relative effect, and the panel surface temperature had no effect.

Huirem and Sahoo [5] analyzed a 17.5 KW LiBr-H<sub>2</sub>O solar-assisted vapor absorption refrigeration system using the Box Behnken Design technique. They studied the impact of generator temperature, LiBr solution concentration, evaporator temperature, and heat exchanger effectiveness on COP, ECOP and TED. Optimal conditions include a 32°C absorber temperature, weak solution concentration of 55.5%, and strong solution concentration of 60%. Increasing heat exchanger effectiveness from 0.5 to 0.9 resulted in a 17.44% increase in COP and ECOP. The model identifies optimum parameters with a COP of 0.79, ECOP of 0.448, and TED of 0.821 kW under specific operational conditions.

S. Agarwal, Arora, and Arora [6] analyzed an absorption-compression cascade refrigeration system (ACCRS) for low-temperature applications. They used an EES software-based model to calculate the system's performance for different temperatures. The triple-effect cascade system saved 45.84% more electricity than the conventional VCR cycle. The COP and exergetic-efficiency of the VCR circuit in the cascade system increased by 85.26% and 85.28%, respectively. The system circulation pump and absorber had the lowest and highest irreversibility.

Azhar and Siddiqui [7] analyzed double-effect parallel flow direct and indirect fired vapor absorption refrigeration systems. They optimized temperatures and solution distribution ratio, comparing parallel and series flow configurations. The study found that the parallel flow cycle had 3-6% higher ECOP and 4% lower EDR than the series flow cycle. The optimum intermediate generator temperature for the parallel flow cycle was significantly lower than the series flow cycle, while the main generator temperature was higher.

In a study by Pandya et al. [8] compared double-effect solar-assisted systems using LiBr-H<sub>2</sub>O and LiCl-H<sub>2</sub>O pairs with ETC and PTC. The study aimed to optimize  $T_{\text{cutoff}}$  and collector type based on Solar COP, Solar exergy efficiency,  $A_{\text{collector}}$ , and product cost. ANOVA revealed the high-temperature condenser's significant impact. LiCl-H<sub>2</sub>O outperformed LiBr-H<sub>2</sub>O in all scenarios. Higher condensation temperatures increased costs and reduced performance. Thermodynamically, LiCl-H<sub>2</sub>O with PTC excelled, though ETC had a 27% smaller collector area. Despite PTC's higher initial cost, economic analysis showed a 17% higher cost for LiCl-H<sub>2</sub>O. However, PTC-based LiCl-H<sub>2</sub>O showed superior Solar COP and efficiency, favoring its integration despite the higher initial product cost.

Talpada and Ramana [9] conducted a review of various studies that focused on modifying absorption systems to improve the performance of absorption refrigeration systems. The study suggests that the performance of absorption refrigeration can be enhanced by using a double-effect and semi-generator absorber solution heat exchanger arrangement. The coefficient of performance of absorption refrigeration can also be improved by combining different refrigeration cycles, such as compression-absorption and ejector-absorption, to form a hybrid refrigeration cycle.

Iffa et al. [10] conducted an exergetic analysis of absorption refrigeration systems using the Design of Experiment approach. They used a Carré Hyper Greco-Latin plan consisting of 16 experiments with the MAPLE computer tool to optimize the coefficient of performance (COP) of the system. The study outcomes suggest that the refrigerating machine with a compressor between the evaporator and the absorber has an acceptable COP. It can operate at a low generator temperature of approximately 60°C while using NH<sub>3</sub>/LiNO<sub>3</sub> as a refrigerant.

Using the Taguchi method, Sivasakthivel et al. [11] optimized a Ground Source Heat Pump's operational parameter. They varied the temperature parameters in three levels and used the "higher the better" concept to obtain a higher coefficient of performance (COP). With a computer program in FORTRAN, they performed computations and analyzed the results using the Signal-to-Noise ratio and Analysis of Variance method. They obtained the maximum COP for heating and cooling operations as 4.25 and 3.32, respectively.

In a study by, M. İ. Karamangil et al. [12] conducted a thorough analysis of absorption refrigeration systems (ARSs) and working fluids. They found that COP values increase with generator and evaporator temperatures, but decrease with condenser and absorber temperatures, as expected. The H<sub>2</sub>O-LiBr mixture system has higher COP values, but has a limited operating range due to crystallization. In contrast, the NH<sub>3</sub>-LiNO<sub>3</sub> solution is more advantageous at low generator temperatures. The study compared the performance of different types of heat exchangers and found that the SHE significantly outperforms the RHE and SRHE, with a maximum increase of 66% in COP.

Prashant et al. [13] employed Taguchi, Grey Relation Analysis, and ANOVA techniques to optimize a Vapor Absorption Refrigeration System (VARS) that utilizes nanoparticles. Their study revealed that incorporating copper-oxide nanoparticles into a VARS system with LiBr-H<sub>2</sub>O as the refrigerant resulted in a 17% increase in the Coefficient of Performance (COP). Among the system parameters, absorber temperature had the most significant impact on performance, followed by evaporator temperature.

Darwish, Al-Hashimi, and Almansoori [14] used Aspen Plus to analyze a Robur ARWA chiller. Aspen Plus provided a flexible platform for analyzing power cycles. The predicted results matched experimental and manufacturer data. The study analyzed performance parameters, including COP, heat duties, refrigerant concentration, and flow rates. The separator heat duty, representing waste heat, affected COP by a maximum of 1.8%. Separator efficiency is key; increasing the number of theoretical stages improved COP by up to 15%. Introducing a throttling process and using stripping gas improved COP by up to 20%.

Jadidi et al. [15] conducted a study to evaluate the performance of a 3.5 kW Solar Ejector Cooling System (SECS) in two office buildings located in different climates using two types of refrigerants, R600a and R290 hydrocarbon. The study involved the development of a mathematical model of the ejector, which is a constant area mixing type, using EES software and the  $\epsilon$ -NTU method, and a simulation program on TRNSYS-EES co-simulator for dynamic study of the cooling cycle. The researchers assessed the thermodynamic energy and exergy of the cooling systems and found that the solar collector system and the ejector component in the cooling cycle were the primary exergy destruction processes. The study also found that R290 (COP = 0.2844) was more efficient in increasing the overall COP of the system than R600a (COP = 0.2797) for the office building located in the semi-arid region.



Using statistical techniques such as DOE, RSM, and ANOVA, this paper aims to establish the foundational context for the ARS. This is because the thermodynamical approach has the limitation of maintaining the other parameter constant when the process involves two or more parameters and the parameter's effect is changed. To determine how operational parameters impact the system's performance characteristics, fewer tests are needed thanks in large part to the statistical technique.

*A. Response Surface Methodology*

Response surface methodology (RSM) is an optimization process technique that entails intricate calculations. Stated differently, the Response Surface Methodology (RSM) comprises a set of statistical and mathematical tools that are helpful for modeling and analyzing situations where a response of interest is affected by multiple variables, with the goal of optimizing this response (Montgomery [16]). For instance, a plant's growth is influenced by specific amounts of sunshine ( $x_2$ ) and water ( $x_1$ ). Under any combination of treatments  $x_1$  and  $x_2$ , the plant can grow. As a result, sunshine and water might change constantly.

The response variable can be developed, enhanced, and optimized with the use of a Response Surface Methodology when treatments are from a continuous range of values. The response variable in this instance is plant growth, or  $y$ , which depends on sunshine and water. It is able to be stated as:

$$y = f(x_1, x_2) + \epsilon \tag{1}$$

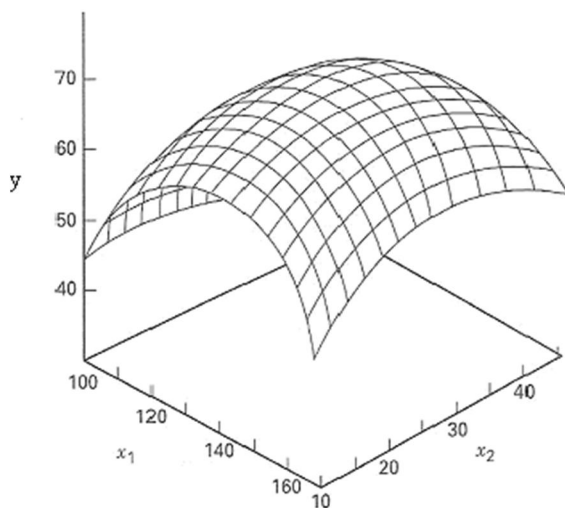


Fig. 1. Response surface plot  
Source: Montgomery et. al (2005)

In this case, the response  $y$  depends on the independent variables  $x_1$  and  $x_2$ .  $y$  is a dependent variable that depends on  $x_1$ ,  $x_2$ , and the experimental error term, represented by the symbol  $\epsilon$ . Any measurement error on the answer and other types of changes not included in  $f$  are represented by the error term  $\epsilon$ . This statistical mistake is thought to have a normal distribution with a mean of zero and a variance of  $\sigma^2$ . The true response function  $f$  is unknown in the majority of RSM cases. A low-order polynomial in a small region is typically the starting point for the researcher as they work to build an accurate approximation for  $f$ . A first-order model is the approximation function if the response is characterized by a linear function of independent variables. Two independent variables in a first-order model can be written as:

$$y = \beta_0 + \beta_1 x_1 + \beta_2 x_2 + \epsilon \tag{2}$$

A higher degree polynomial has to be utilized if the response surface is curved. A second-order model is the approximation function that has two variables:

$$y = \beta_0 + \beta_1 x_1 + \beta_2 x_2 + \beta_{11} x_1^2 + \beta_{22} x_2^2 + \beta_{12} x_1 x_2 + \epsilon \tag{3}$$

Generally speaking, one or a combination of these two models is used in all RSM problems. Every factor's level in each model is unrelated to the levels of the other components. When creating an RSM model, a mixed model is useful if the levels of each factor are not independent.

Data collection requires the use of an appropriate experimental design in order to yield the most efficient outcome in the approximation of polynomials. The parameters of the polynomials are estimated using the Method of Least Squares after the data have been gathered.

The fitted surface is used to carry out the response surface analysis. Designs for fitting response surfaces are under the category of response surface designs. Thus, the goal of researching RSM can be achieved through:

- 1) Understanding the topography of the response surface (local maximum, local minimum, ridge lines), and
- 2) Finding the region where the optimal response occurs. The goal is to move rapidly and efficiently along a path to get to a maximum or a minimum response so that the response is optimized.

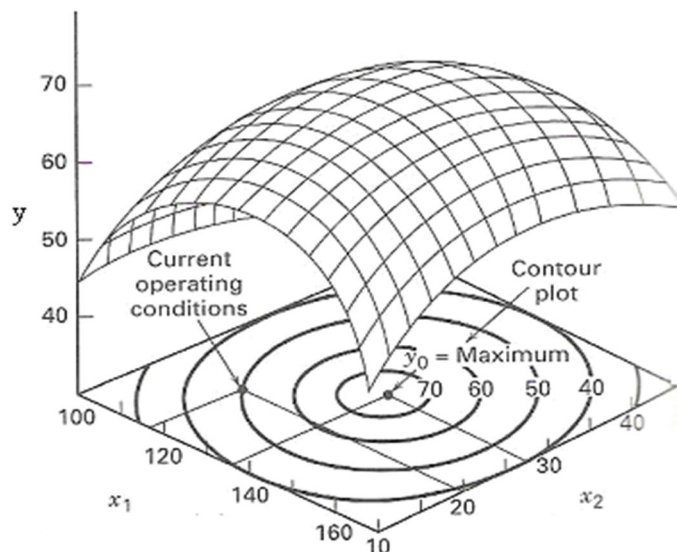


Fig. 2: Contour plot

Using the data input from the experiment, the RSM technique builds an appropriate experimental design that integrates all of the independent variables and ultimately produces a set of equations that may theoretically determine the value of an output. Regression analysis with a well-designed base on the controlled values of independent variables yields its outcomes. Following that, predictions about the dependent variable can be made using the updated values of the independent variables. When Box and Wilson originally proposed RSM in 1951, there were a lot fewer experimental runs than there were when complete factorial design was used. Consequently, it has been modified for use in several studies, such as those conducted in the dairy and other industries, where Solanki et al. [17] provides a detailed explanation of the technical procedures. In addition to fewer experimental runs, the RSM results are said to be statistically significant. The laboratory test step is made more effective by using the RSM approach in the optimization process, which reduces the amount of time needed to test all the factors related to the customer evaluation. Furthermore, parameters estimation can be used to pinpoint the variables that are significantly impacting the model, allowing researchers to concentrate on the specific variables that influence the acceptability of the product. In an experimental design, a factor or process variable can typically depend on another variable or be dependent upon it. To determine the output-input relationship, it is essential to understand how the elements interact. This explains why the one-factor-at-a-time method is rarely used to determine the interactions. Using quantitative data, RSM may create a model equation to assess the relationship and interactions between the various components. Kazemian et al. [18]. Implementing RSM involves three steps: (1) experiment design, such as Box Behnken and Central Composite Design (CCD); (2) statistical and regression analysis to create model equations representing response surface modeling; and (3) model equation-based parameter and variable optimization. In order to optimize the layout of dynamic facilities, Goyal et al. [19] and Gambhir et al. [20] utilized RSM. The presence of a maximum, minimum, or saddle point in the system is a crucial feature that is of great relevance to the industry. RSM is therefore being utilized in the market more and more. Additionally, the chemical and processing fields have recently focused more on identifying areas where responsiveness has improved than on determining the ideal response (Myers, Khuri, and Carter [21]). As a result, RSM development and application will be utilized in a variety of contexts in the future.

## II. SYSTEM DESCRIPTION

A model for a single-effect vapor absorption system is presented in Figure 3. The system encompasses essential components, including an absorber, a generator, a condenser, an evaporator, a solution heat exchanger (SHE), a refrigerant heat exchanger (RHE), a solution expansion valve, a pump, and a refrigerant expansion valve. The system operates through two circuits: the refrigerant circuit and the LiBr–H<sub>2</sub>O solution circuit. Heat is introduced into the generator ( $Q_g$ ), initiating the evaporation of the refrigerant H<sub>2</sub>O at high pressure ( $P_c$ ). The evaporated H<sub>2</sub>O is then transported to the condenser, where it releases heat ( $Q_c$ ), leading to the phase change of H<sub>2</sub>O from vapor to liquid.

Subsequently, the refrigerant H<sub>2</sub>O is directed to the refrigerant expansion valve (RTV) via a refrigerant heat exchanger to achieve evaporation pressure ( $P_e$ ), resulting in passage to the evaporator. In the evaporator, the cooling process occurs as the refrigerant absorbs heat ( $Q_e$ ) from the environment, prompting the refrigerant to evaporate once again before entering the absorber. Here, it blends with the weak solution from the generator, forming a LiBr–H<sub>2</sub>O solution with reduced concentration and releasing heat ( $Q_a$ ). The solution is then pumped to the generator, attaining condenser pressure ( $P_c$ ) through a solution heat exchanger, elevating its temperature.

The cycle commences once a sufficient temperature is achieved in the generator. A portion of the refrigerant evaporates, proceeding to the condenser. The remaining solution, characterized by high concentration, undergoes cooling in the heat exchanger, followed by passage through a throttle valve (STV) where its pressure decreases to the evaporation pressure ( $P_e$ ).

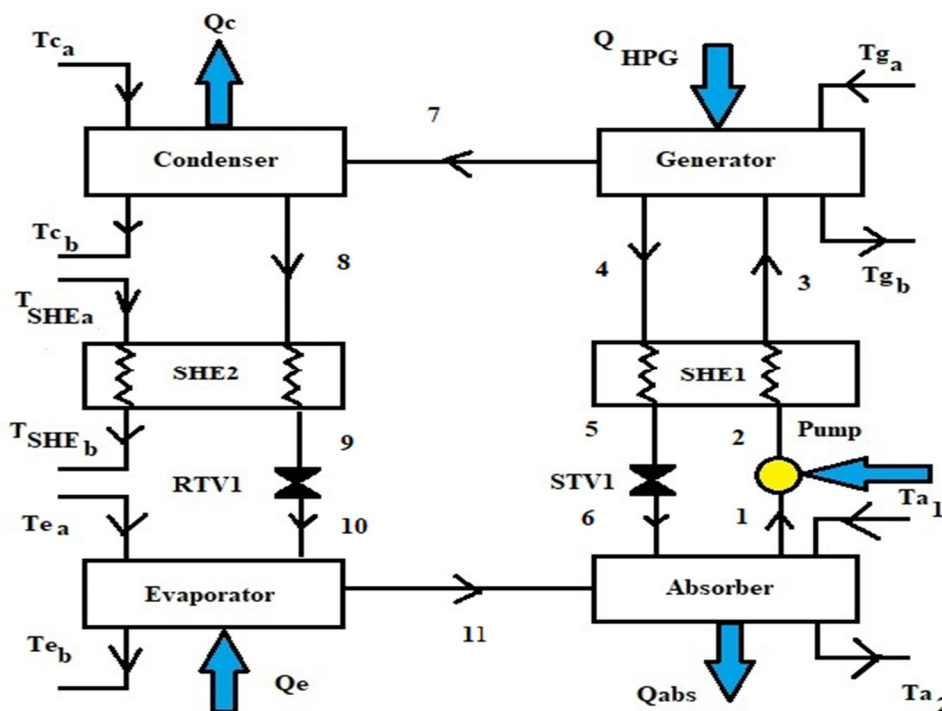


Fig.3 Schematic of single stage vapor absorption system

## III. METHODOLOGY ADOPTED

A thermodynamic optimization analysis of a 1-ton capacity single-effect LiBr–H<sub>2</sub>O vapor absorption cooling system is conducted, employing both first and second-law principles. Mathematical models, derived from thermodynamics theory, are implemented in the Engineering Equation Solver (EES) for the computational process. The determination of the minimum generator temperature, a critical parameter for system operation, has been accomplished. The study involves a comprehensive comparison of thermodynamic analyses based on the first and second laws.

The primary method for enhancing the efficiency of an absorption cycle is through thermodynamic analysis and optimization. Consequently, the present investigation adopts first-law and second-law-based thermodynamic analyses to optimize the system's performance. A realistic comparison between the first and second law perspectives is conducted, aiming to guide the design of an optimum system.

The main emphasis of this study is on identifying the optimum generator temperature from both energy and exergy perspectives. Simultaneously, the minimum generator temperature required for system operation is also evaluated. Objective parameters such as the Coefficient of Performance (COP) and exergy destruction rate are selected, and the influence of condenser and evaporator temperatures on the optimum generator temperature is examined. Following the numerical simulation of the single-stage LiBr-water absorption system using the EES computer code and ensuring computational accuracy, the determination of an appropriate mathematical model becomes crucial for investigating the role of each desired parameter. To achieve this, a response surface methodology is employed, utilizing Box-Behnken Design (BBD) within the framework of advanced Design of Experiments (DOE) techniques for a more comprehensive understanding and optimization of the system's response.

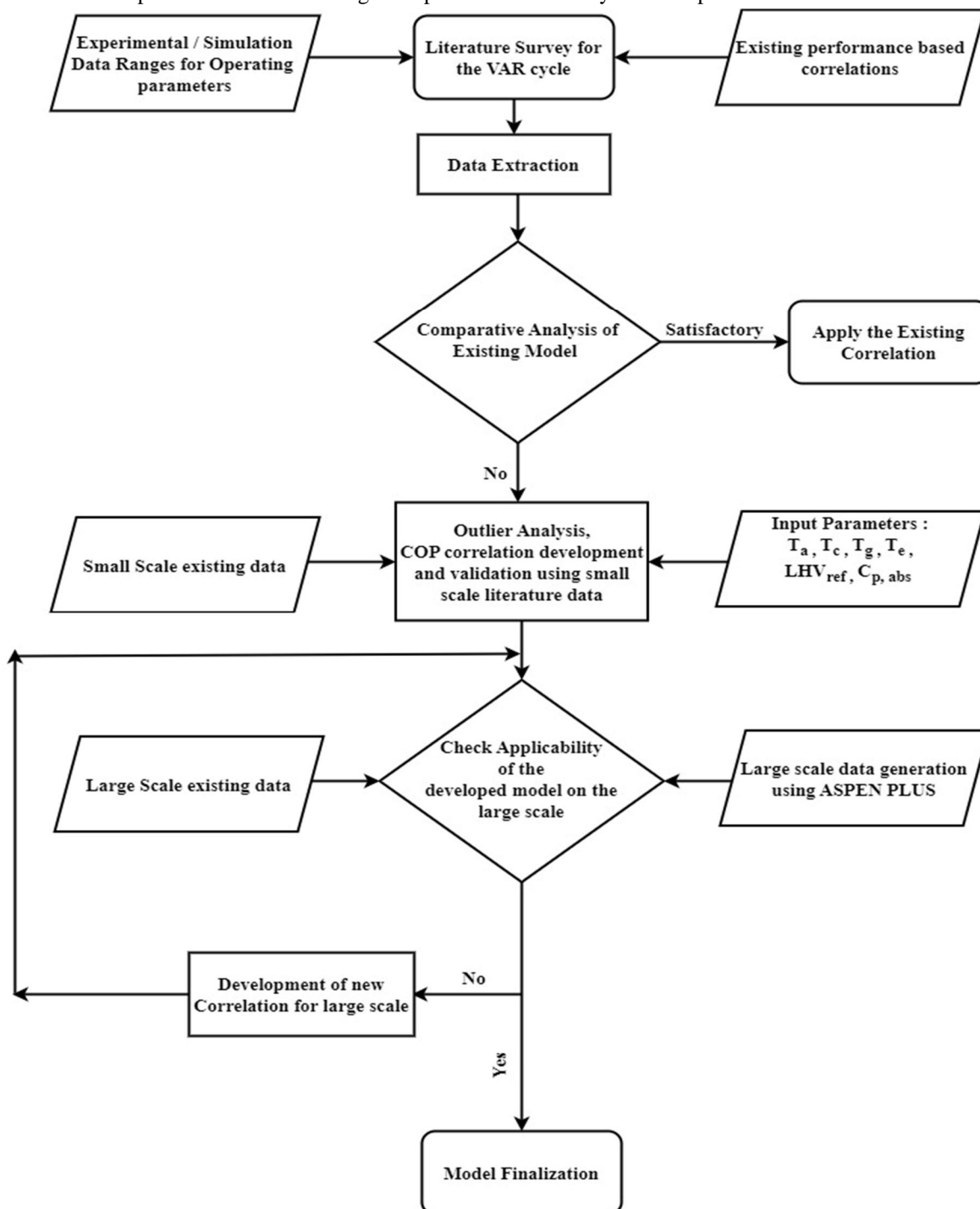


Fig.4 Schematic of RSM approach for COP Correlation development of VARs.

#### IV. MATHEMATICAL MODELLING

The basic equations used in the analysis of the first laws of thermodynamics are presented here:

$$\sum m_i - \sum m_o = 0 \tag{4}$$

$$\sum m_i X_i - \sum m_o X_o = 0 \tag{5}$$

where,  $m$  is the mass flow rate and  $X$  is the mass fraction of LiBr in the solution.

Using Eq. (4) and (5), the mass balancing of particular element of the absorption mechanism has been advanced as:

Generator:

$$m_3 = m_4 + m_7 \tag{6}$$

$$m_3 X_3 = m_4 X_3 + m_7 X_3 \tag{7}$$

Condenser:

$$m_7 = m_8 \tag{8}$$

RHE:

$$m_8 = m_9 \tag{9}$$

RTV:

$$m_9 = m_{10} \tag{10}$$

Evaporator:

$$m_{10} = m_{11} \tag{11}$$

Absorber:

$$m_1 = m_{11} + m_6 \tag{12}$$

Pump:

$$m_1 = m_2 \tag{13}$$

SHE:

$$m_2 = m_3 \tag{14}$$

$$m_4 = m_5 \tag{15}$$

STV:

$$m_5 = m_6 \tag{16}$$

The first law of thermodynamics for each component of the absorption system is expressed as follows:

$$\sum \dot{Q} - \sum \dot{W} = \sum m_o h_o - \sum m_i h_i \tag{17}$$

Energy equilibrium equations of different components of absorption system are as:

Condenser:

$$Q_c = m_7(h_7 - h_8) = m_c(h_{cb} - h_{ca}) \tag{18}$$

RHE:

$$Q_{RHE} = m_8(h_8 - h_9) = m_{RHE}(h_{RHEb} - h_{RHEa}) \tag{19}$$

Evaporator:

$$Q_e = m_{11}(h_{11} - h_{10}) = m_e(h_{ea} - h_{eb}) \tag{20}$$



Absorber:

$$Q_a = m_{11}h_{11} + m_6h_6 - m_1h_1 = m_a(h_{a2}-h_{a1}) \quad (21)$$

Pump:

$$W_p = m_1v_1(P_2 - P_1)/1000 \quad (22)$$

SHE:

$$Q_{SHE} = m_3(h_3-h_2) = m_5(h_4 - h_5) \quad (23)$$

Generator:

$$Q_g = m_3h_3 + m_7h_7 - m_4h_4 = m_g(h_{g2}-h_{g1}) \quad (24)$$

The overall performance of the absorption system has been determined by evaluating its coefficient of performance (COP) as:

$$COP = \frac{Q_e}{Q_{HTG} + W_p} \quad (25)$$

where,  $Q_e$  is the refrigerant effect,  $Q_{HTG}$  is the heat rate in the generator, and  $W_p$  is the pump work.

### B. Assumptions for Thermodynamic Analysis

For this part we established a thermodynamic analysis of the single-effect machine with a heat exchanger operating with the pair ( $H_2O/LiBr$ ).

We adopt the following assumptions.

- 1) There is saturated refrigerant at the condenser and evaporator outlets.
- 2) There is no departure of chemical substances from the cycle to the environment.
- 3) The kinetic and potential energy effects are neglected.
- 4) The refrigerant (water) at the outlet of the condenser is saturated liquid and vapour.
- 5) The Lithium bromide solution at the absorber outlet is a strong solution and it is at the absorber temperature.
- 6) The outlet temperatures from the absorber and from generators correspond to equilibrium conditions of the mixing and separation respectively.
- 7) Pressure losses in the pipelines and all heat exchangers are negligible.
- 8) Heat exchange between the system and surroundings, other than in that prescribed by heat transfer at the generator, evaporator, condenser and absorber, does not occur.

### C. Parameters and Levels

Four factors, including generator, evaporator, condenser, and absorber temperatures, are taken into account in this study to optimize the absorption refrigeration system. The literature review is used to determine the parameter levels, as Table 1 illustrates. By utilizing Box-Behnken design, the RSM technique maximizes system performance. A great deal of phenomena in engineering are based on hypotheses, and as a result, some of them are too complex to adequately capture mathematically, either because of unidentified mechanisms, a high number of governing factors, or both. In the design of experiments and engineering related sciences, response surface methodology (RSM) is one of the exploration methodologies.

It is a collection of statistical and mathematical techniques that are useful for modeling and analyzing issues where multiple variables influence the response parameter and are optimized. Using an appropriate test design, this technique looks for a way to estimate interactions, quadratic effects, and even the localized surface of the response. Following EES's numerical simulation of the single-stage LiBr-water absorption system in computer code and verification of the results' accuracy, the right mathematical model must be chosen in order to examine the significance of each desired parameter. A collection of sophisticated design of experiments (DOE) methods called response surface methodology aids in the improved comprehension and optimization of response.

One advantage of the Box-Behnken design is that it assumes fewer runs for three components. This benefit vanishes for four or more components. Although the Box-Behnken design can be rotated, some regions, like CCI, have low prediction quality. The experimenter may be prevented from overdoing the combination of elements by its "missing corners." The selection of the parameters and their design ranges is the next step. The parameter ranges (taken from Canbolat [22]) for the COP analysis are displayed in Table 1.

Table 1: Ranges of parameters for the analysis on the COP

Parameters	Levels		
	-1	0	1
Generator temperature, T <sub>g</sub>	90	110	130
Condenser temperature, T <sub>c</sub>	28	33	38
Absorber temperature, T <sub>a</sub>	28	33	38
Evaporator temperature, T <sub>e</sub>	-5	2.5	10

D. COP Estimation

According to equations (4) to (25), a computational computer code was written in EES based on input parameters introduced in Table 2 to study the coefficient of performance of the cycle.

Table 2: COP results

Run	T <sub>g</sub>	T <sub>c</sub>	T <sub>a</sub>	T <sub>e</sub>	COP
1	130	38	33	2.5	0.85
2	90	28	33	2.5	0.91
3	110	38	28	2.5	0.86
4	90	33	33	10	0.90
5	110	33	28	-5	0.863
6	90	33	28	2.5	0.883
7	90	38	33	2.5	0.799
8	110	33	38	-5	0.817
9	110	33	38	10	0.904
10	90	33	33	-5	0.72
11	130	33	33	-5	0.838
12	90	33	38	2.5	0.833
13	130	33	28	2.5	0.863
14	110	28	28	2.5	0.902
15	130	33	38	2.5	0.863
16	110	38	33	-5	0.802
17	110	28	33	10	0.909
18	110	28	38	2.5	0.905
19	110	33	28	10	0.887
20	130	33	33	10	0.870
21	110	28	33	-5	0.875
22	110	33	33	2.5	0.888
23	110	33	33	2.5	0.888
24	130	28	33	2.5	0.870
25	110	38	38	2.5	0.853
26	110	38	33	10	0.881

V. RESULTS AND DISCUSSION

A. Results Validation

EES code validation has been done by comparing the results of the current simulation with those of Ketfi et al. [23], Kaushik et al. [24], and Modi et al. [25] before moving on to statistical analysis. Table 3 presents a comparison of the results of the simulation. In comparison to Ketfi et al. [23], the COP divergence is -2.83%.

Comparing the current simulation results with those of Modi et al. [25] and Kaushik et al. [24], we find that the variation in COP is +6.63% and +6.71%, respectively. The irreversibility distribution among each component of the absorption process accounts for the diversity in findings. Furthermore, the simulation works satisfactorily with the existing single-impact vapor absorption system.

Table 3: Comparison of validation results of COP with the published literature

Sr. No.	Published literature	T <sub>g</sub> (°C)	T <sub>c</sub> (°C)	T <sub>a</sub> (°C)	T <sub>e</sub> (°C)	COP	COP Estimated using EES code	Deviation
1	Ketfi et al. [23]	90	40	40	7	0.775	0.753	-2.83%
2	Modi et al. [25]	87.8	37.8	37.8	7.2	0.7615	0.812	6.63%
3	Kaushik et al. [24]	87.8	37.8	37.8	7.2	0.7609	0.812	6.71%

**B. ANOVA Results and Regression Model**

Determination coefficient R<sup>2</sup>, adjusted R<sup>2</sup>, predicted R<sup>2</sup>, and coefficient of variation (CV%) were determined to check the adequacy and accuracy of the developed models. The R<sup>2</sup> indicates the proportion of the total variation in the response predicted by the models. The higher correlation coefficients confirm the suitability of the models and correctness of the calculated constants.

Table 4: ANOVA table and statistical parameters of quadratic model

Source	Sum of Squares	df	Mean Square	F-value	p-value	
Model	0.0344	9	0.0038	110.62	< 0.0001	Significant
A-T <sub>g</sub>	0.0080	1	0.0080	230.55	< 0.0001	
B-T <sub>c</sub>	0.0053	1	0.0053	154.22	< 0.0001	
C-T <sub>e</sub>	0.0161	1	0.0161	465.64	< 0.0001	
AB	0.0005	1	0.0005	15.73	0.0027	
AC	0.0016	1	0.0016	47.17	< 0.0001	
BC	0.0008	1	0.0008	22.33	0.0008	
A <sup>2</sup>	0.0008	1	0.0008	22.87	0.0007	
B <sup>2</sup>	0.0001	1	0.0001	1.62	0.2313	
C <sup>2</sup>	0.0015	1	0.0015	42.64	< 0.0001	
Residual	0.0003	10	0.0000			
Lack of Fit	0.0003	5	0.0001			
Pure Error	0.0000	5	0.0000			
Cor Total	0.0347	19				

The **Model F-value** of 110.62 implies the model is significant. There is only a 0.03% chance that an F-value this large could occur due to noise. **P-values** less than 0.05 indicate model terms are significant. In this case A, B, C, AB, AC, BC, A<sup>2</sup>, C<sup>2</sup> are significant model terms. The ANOVA of the quadratic regression model demonstrates that the model was highly significant. This was evident from the Fisher’s F-Test (F value=110.62) and a low probability value (p=0.0003). The CV% obtained is 0.65 for the response. The low value of CV% indicates the degree of precision with which the simulation is carried out. A low value of CV% suggests a high reliability of the experiment. Adequate precision value measures the signal-to-noise ratio, and a ratio greater than 4 is generally desirable which indicates adequate model discrimination. The adequate precision value obtained in this study is 12.13 which indicated adequate signal.

Table 5: Statistical data of quadratic model

Std. Dev.	0.0059	R <sup>2</sup>	0.9901
Mean	0.8956	Adjusted R <sup>2</sup>	0.9811
C.V. %	0.6559	Predicted R <sup>2</sup>	0.9159
+			
		Adeq. Precision	38.2967

The empirical relationship between the simulation results obtained is expressed by a second-order polynomial equation and the equation arrived for coded factors is given by the eqn (26).

$$COP = 0.908858305582 + 0.024133930102172 A - 0.019738899025539 B + 0.03429826036581 C + 0.0082374999999999 AB - 0.0142625 AC + 0.0098125 BC - 0.0073990929138372 A^2 - 0.0019720483682305 B^2 - 0.010103776351876 C^2 \quad (26)$$

C. Comparison Between Predicted and Simulation Values

To determine whether the fitted model was a sufficient approximation to the actual values, the model's conformation was performed. The optimization of the fitted response surface is likely to produce poor or misleading results unless the model demonstrates a reasonable match. The diagnostic charts, which show predicted values against simulation results, were used to verify the model's satisfactoriness. The relationship between the experimental and anticipated values was also displayed in the charts. Fig. 5 displays the response's diagnostic plots. There was sufficient agreement between the actual data and the data derived from the models, as seen by the data points on this plot that reasonably approached the straight line. The normality of the residuals was checked by analyzing the data. The normal probability plot shown in Fig. 6 depicts the normal distribution of the residuals. The residuals provide the difference between the observed value of a response and the value that is fitted under the theoretical model. The small residual value indicates that the model prediction is accurate. The data points lie reasonably close to straight line in Fig.5. Some scatter was also found with normal data and it could be concluded that the data are normally distributed.

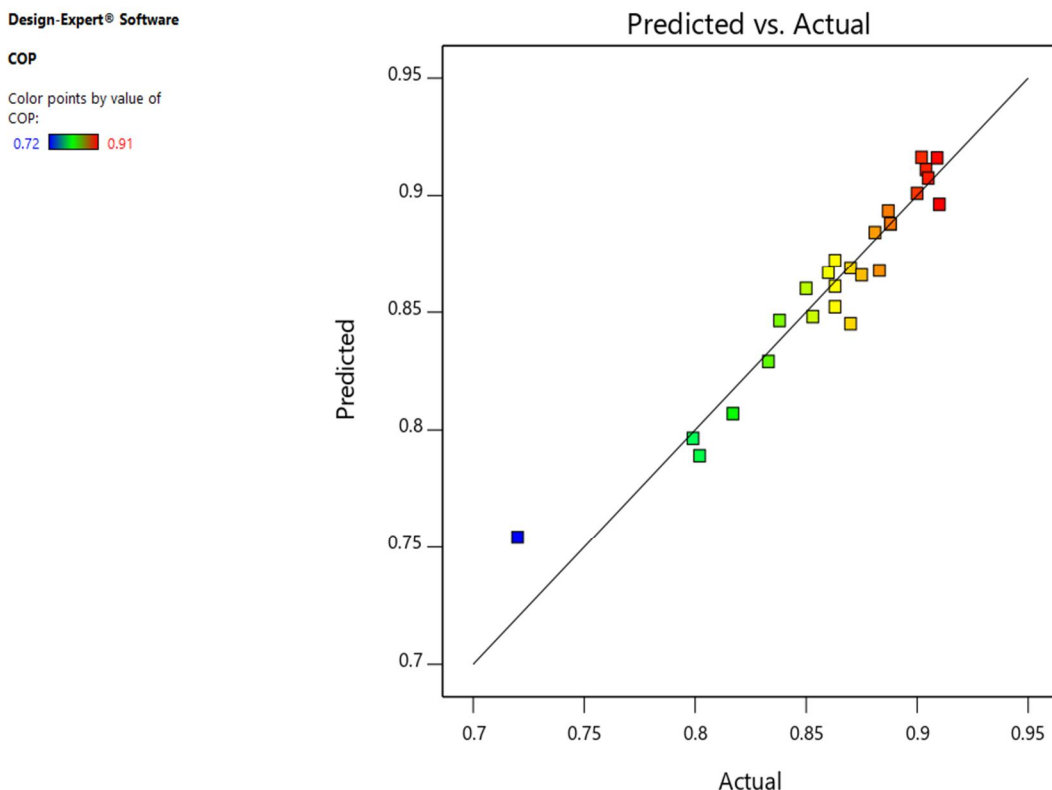


Fig. 5: Comparison between predicted and simulation values



As seen in Fig. 6, the plots of residual for COP are randomly distributed and not followed by any ordered pattern. Hence, it can be derived that the residual analysis does not demonstrate any model inadequacy or the model is suitable for predicting the responses at a confidence level of 95%.

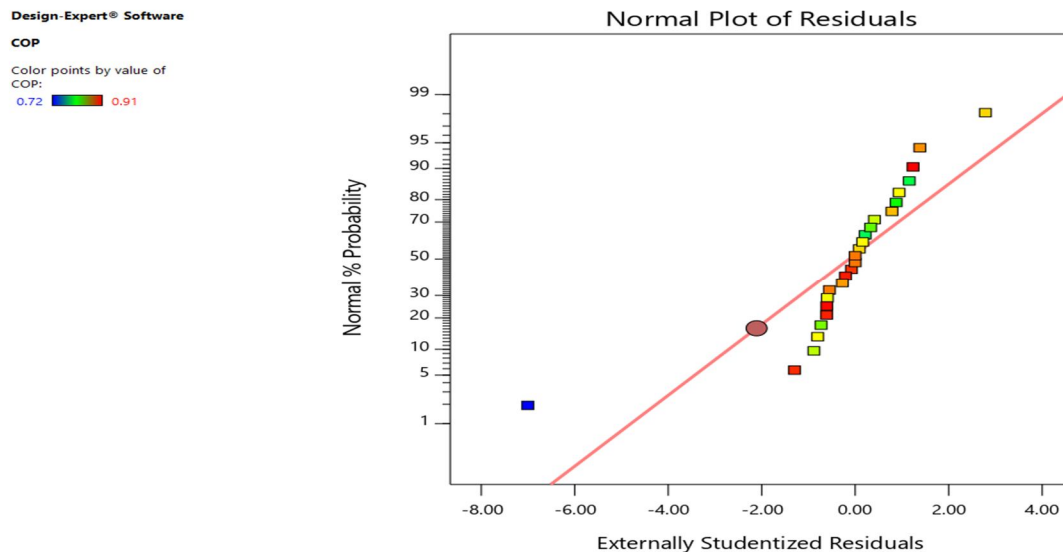


Fig. 6: Normal probability plots of standardized residuals

**D. Interaction Between the Operational Variables**

To show how operational parameters affect response function, two-dimensional contours based on quadratic models generated in terms of the input factors (actual variables) to predict the COP as response functions are displayed and explained in figures between 7 and 12. The influence of various independent elements can be better understood with the aid of the 2D outlines. The response surface of the COP is shown in Figure 7 as a function of the temperatures of the generator and condenser. Making a map of response values as a function of input parameters is one of the most fascinating aspects of the RSM. To help visualize the expected model equation, response surface plots might be used. In addition, the response surfaces were represented as two-factor three-dimensional plots, while the other components remained unchanged.

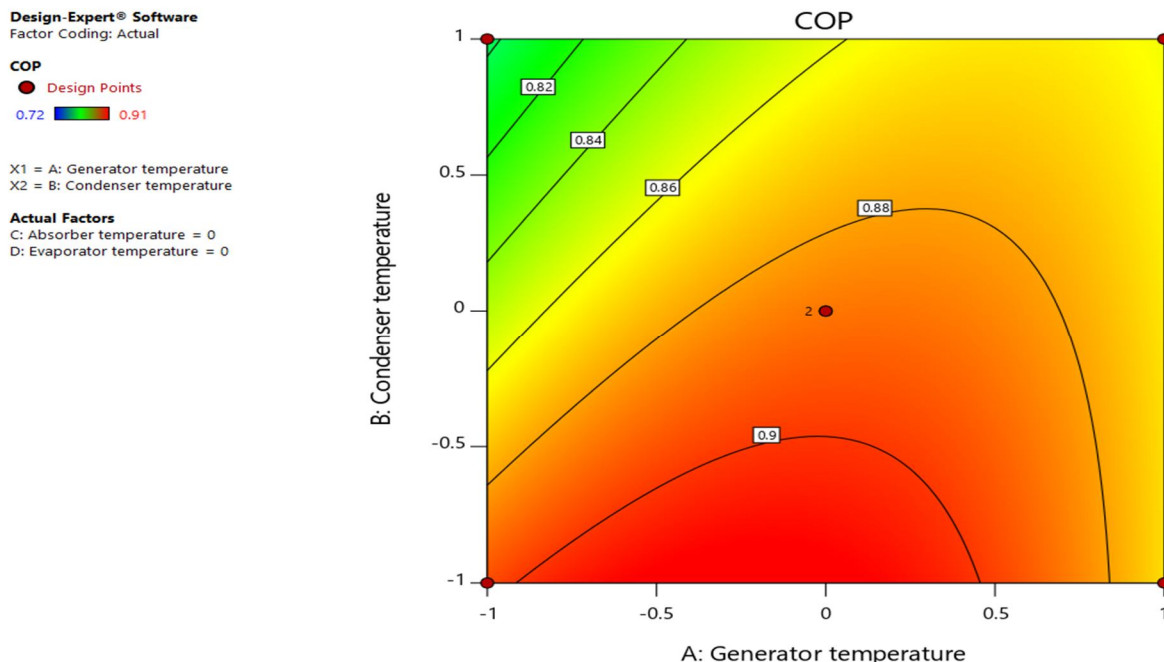


Fig. 7: Effect of generator and condenser temperature on COP

**Design-Expert® Software**  
Factor Coding: Actual

**COP**  
● Design Points  
0.72 0.91

X1 = A: Generator temperature  
X2 = C: Absorber temperature

**Actual Factors**  
B: Condenser temperature = 0  
D: Evaporator temperature = 0

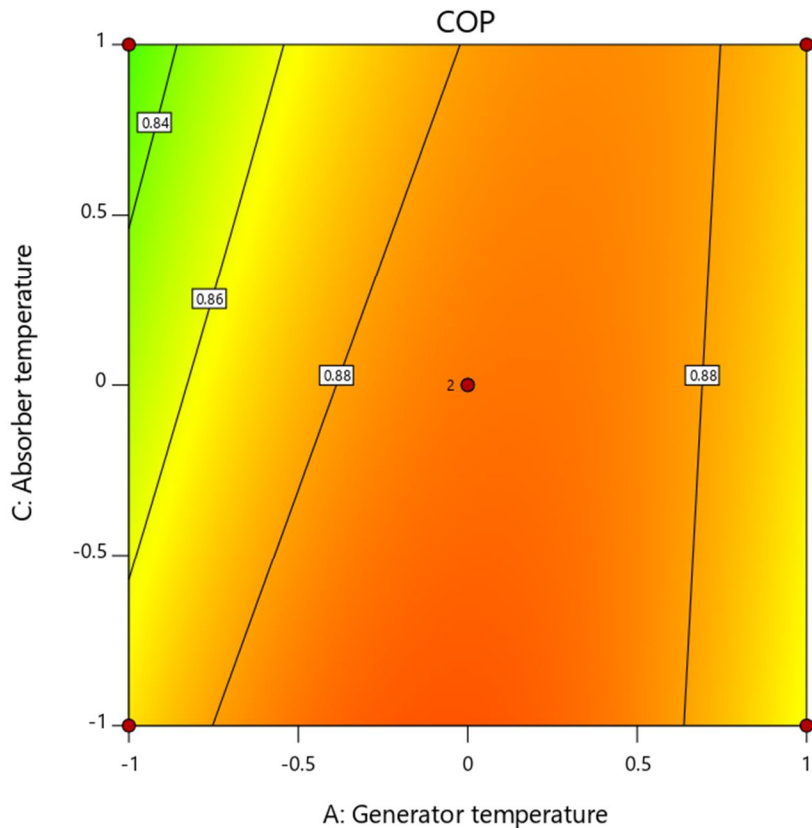


Fig. 8: Effect of generator and absorber temperature on COP

**Design-Expert® Software**  
Factor Coding: Actual

**COP**  
● Design Points  
0.72 0.91

X1 = A: Generator temperature  
X2 = D: Evaporator temperature

**Actual Factors**  
B: Condenser temperature = 0  
C: Absorber temperature = 0

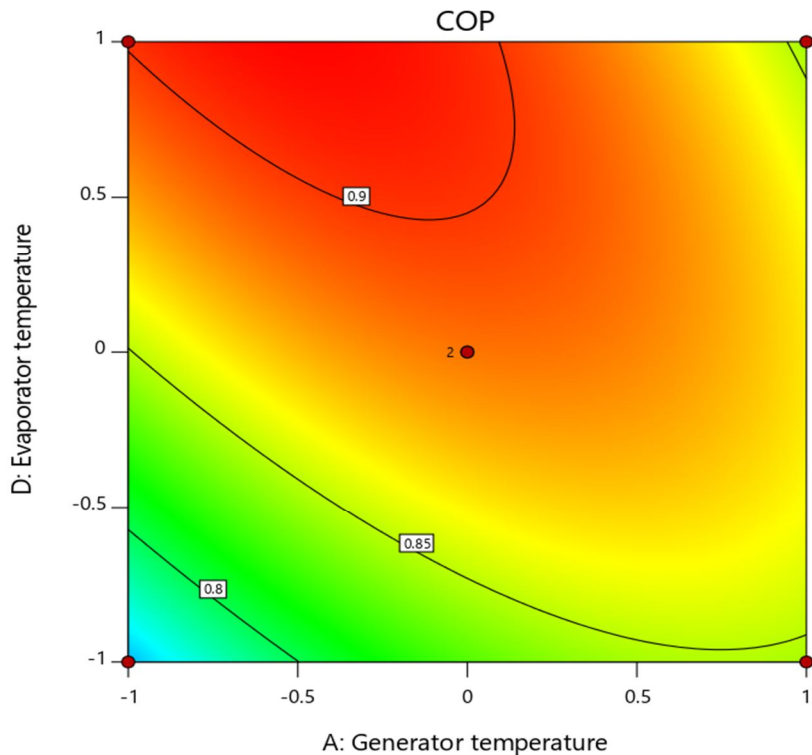


Fig. 9: Effect of generator and evaporator temperature on COP

**Design-Expert® Software**  
Factor Coding: Actual

**COP**  
● Design Points  
0.72 0.91

X1 = B: Condenser temperature  
X2 = C: Absorber temperature

**Actual Factors**  
A: Generator temperature = 0  
D: Evaporator temperature = 0

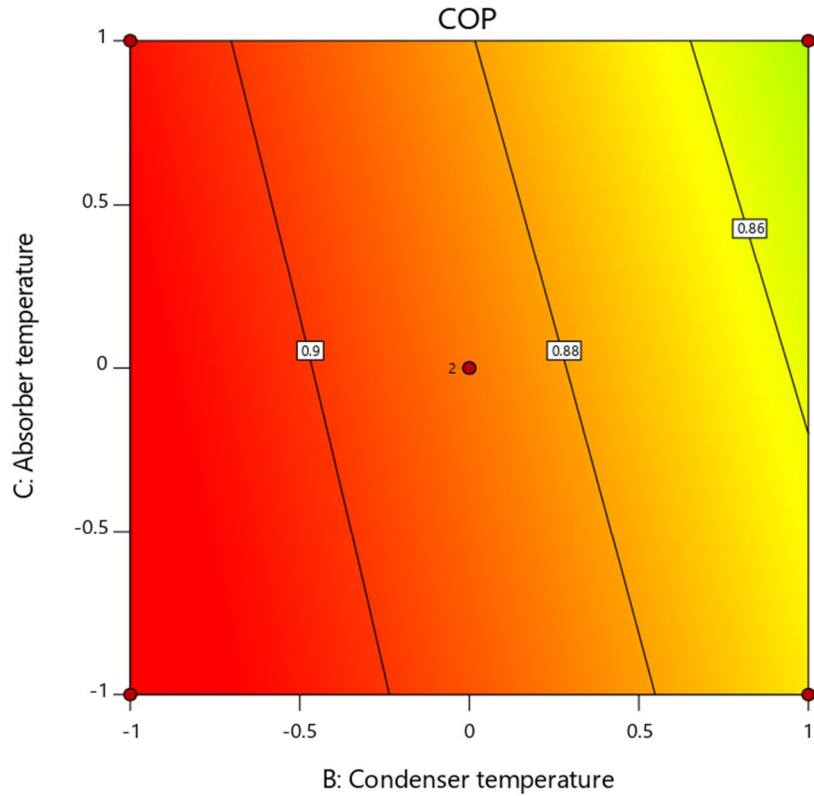


Fig. 10: Effect of condenser and absorber temperature on COP

**Design-Expert® Software**  
Factor Coding: Actual

**COP**  
● Design Points  
0.72 0.91

X1 = B: Condenser temperature  
X2 = D: Evaporator temperature

**Actual Factors**  
A: Generator temperature = 0  
C: Absorber temperature = 0

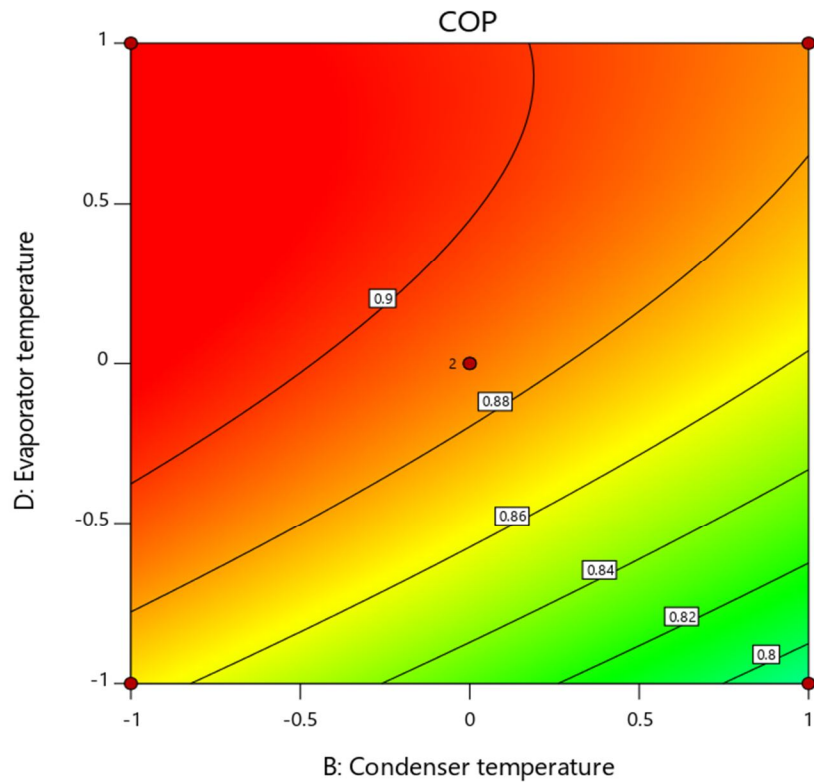


Fig. 11: Effect of condenser and evaporator temperature on COP

**Design-Expert® Software**  
Factor Coding: Actual

**COP**  
● Design Points  
0.72 0.91

X1 = C: Absorber temperature  
X2 = D: Evaporator temperature

**Actual Factors**  
A: Generator temperature = 0  
B: Condenser temperature = 0

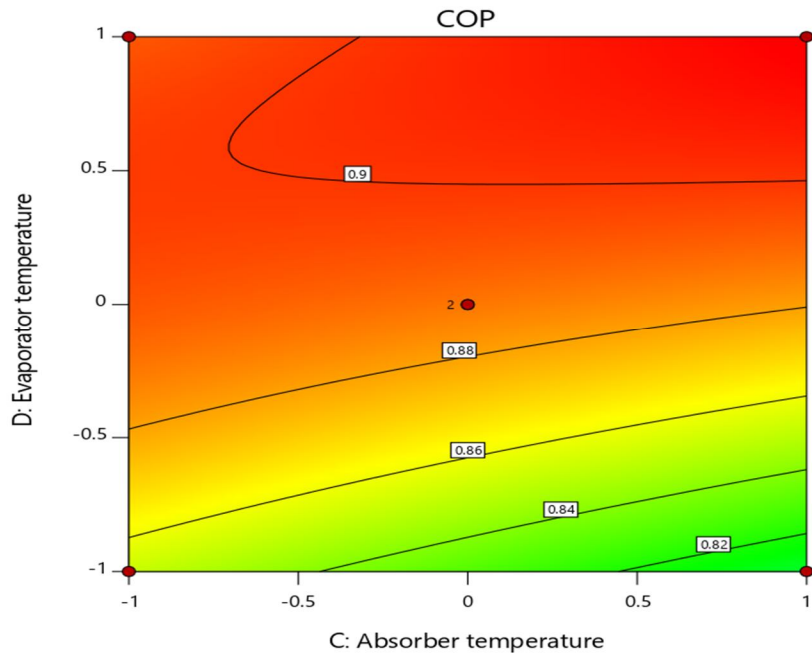


Fig. 12: Effect of absorber and evaporator temperature on COP

*E. Selection of Optimum Conditions*

The study has successfully identified optimal conditions for achieving maximum Coefficient of Performance (COP). Utilizing second-order polynomial models developed for each response, the investigation focused on determining specific optimum conditions. Having defined the most significant parameters in prior analyses, the subsequent phase involved pinpointing the optimal values for these parameters that would result in the highest COP. For this purpose, Derringer's desirability function method was employed for the optimization of multiple responses. Figure 12 illustrates the optimized conditions for COP, and the attained optimum COP value is recorded as 0.716.

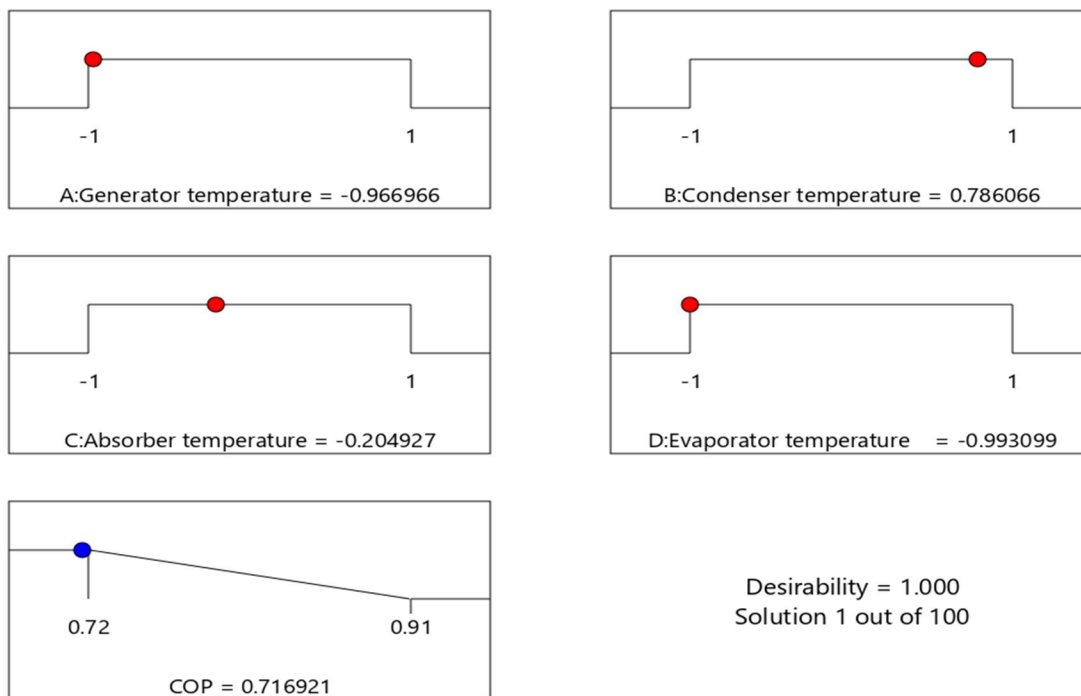


Fig. 12: Optimum parameter plot



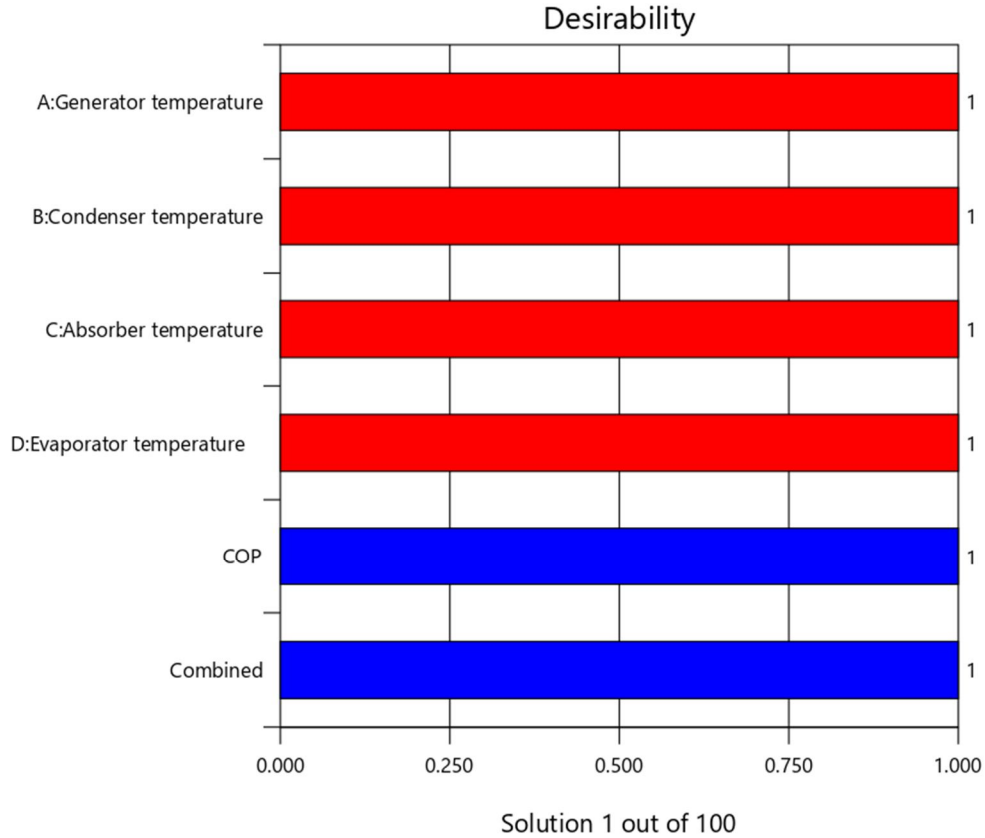


Fig. 13: Desirability plot

Design-Expert® Software  
Factor Coding: Actual

All Responses

Actual Factors

A: Generator temperature = -0.966966  
B: Condenser temperature = 0.786066  
C: Absorber temperature = -0.204927  
D: Evaporator temperature = -0.993099

Responses

Desirability = 1  
COP = 0.716921

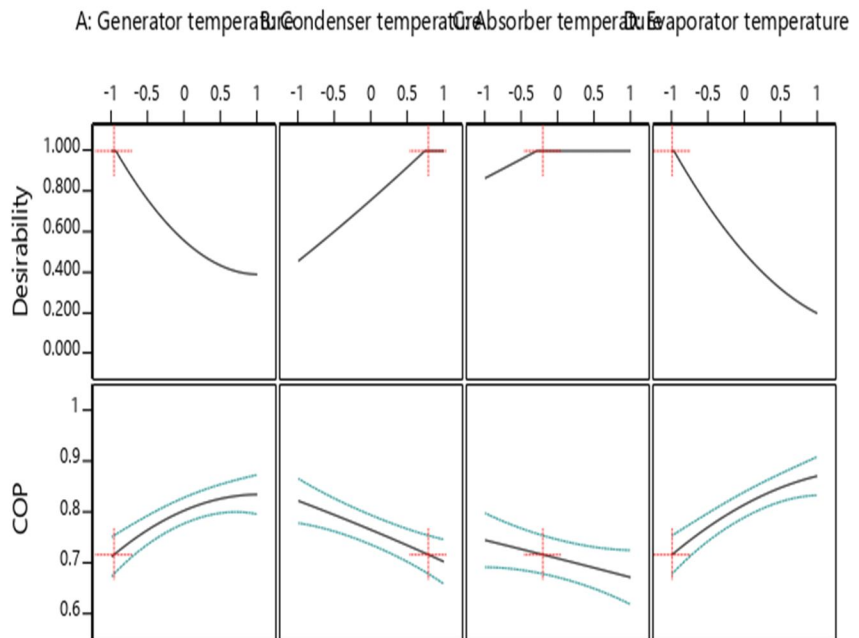


Fig. 14: Effect of parameters on COP

With increase in generator and evaporator temperature, COP increases while increase in condenser and absorber temperature COP decreases.

Design-Expert® Software  
Factor Coding: Actual

All Responses

Actual Factors

A: Generator temperature = -0.966966  
B: Condenser temperature = 0.786066  
C: Absorber temperature = -0.204927  
D: Evaporator temperature = -0.993099

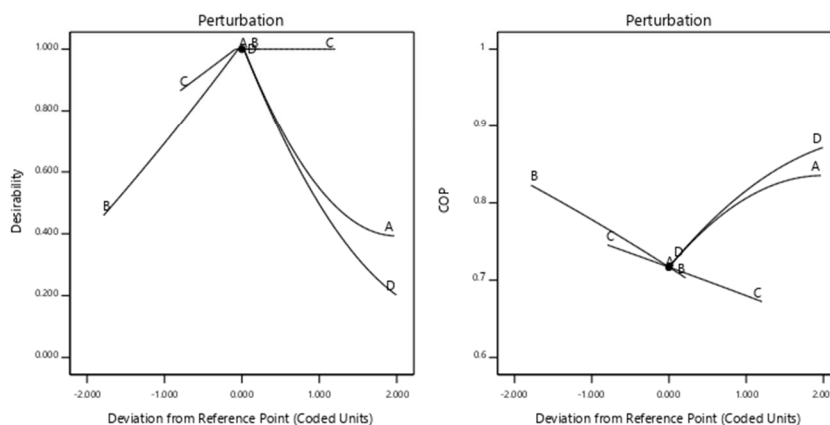


Fig. 15: Perturbation plot on COP

In Figure 15 the perturbation plot is shown. It predicts the effects of all factors at the midpoint of the design. It can be predicted that changes in the variables with a steeper positive slope have a higher direct relation with response function. Changes in variables with a steeper negative slope have a higher inverse effect on response function.

## VI. CONCLUSION

In the current study, Response Surface Methodology (RSM) designs, such as Box-Behnken Design (BBD), are employed for fitting quadratic equations and subsequently compared. Specifically, the BBD method within RSM is applied to investigate the influential parameters in the LiBr-water absorption refrigerant system. The simulation code for the LiBr-water absorption refrigerant system is explored in Engineering Equation Solver (EES), considering variations in maximum/minimum pressure, solution concentration, pure ammonia content, isentropic efficiency of the pump, mass flow rate, and effectiveness factor of the heat exchanger. An analysis of variance (ANOVA) is conducted to assess the impact of various factors on the coefficient of performance.

The ANOVA results for the quadratic regression model indicate its high significance, substantiated by the Fisher's F-Test ( $F$  value=9.77) and a low probability value ( $p=0.0003$ ). The Coefficient of Variation (CV%) is found to be 2.04 for the response variable, signifying a high precision in the simulations. A low CV% suggests reliable experimentation. The Adequate Precision value, measuring the signal-to-noise ratio, is 12.13, exceeding the desirable ratio of 4, indicating sufficient model discrimination.

Comparisons with the work by Canbolat et al [22] involving Taguchi and ANOVA methods reveal the determined importance order of parameters. Under operating conditions, the best Coefficient of Performance (COP) calculated in our study using the RSM technique is 0.716, surpassing the value obtained through Taguchi-Grey Relational Analysis (GRA) in Canbolat's study, which was 0.6255. Furthermore, the study highlights the impact of generator and evaporator temperature increase on COP enhancement, while an increase in condenser and absorber temperature results in COP reduction. Optimization using Derringer's desirability function method yields an optimum COP value of 0.716.

## VII. FUTURE SCOPE OF WORK

Considering the comprehensive analysis conducted in the current study, the following future scope of work is proposed:

- 1) *Integration of Advanced Materials:* Investigate the impact of incorporating advanced materials in the components of the LiBr-water absorption refrigerant system. This could include exploring materials with enhanced thermal conductivity, corrosion resistance, and durability to improve overall system efficiency.
- 2) *Dynamic Simulation Studies:* Extend the scope by incorporating dynamic simulation studies to capture transient behaviors and responses of the system under varying operating conditions. Dynamic modeling can provide insights into the system's performance during start-up, shut-down, and transient states.

- 3) *Environmental Impact Assessment*: Evaluate the environmental impact of the LiBr-water absorption refrigerant system. Assess the system's carbon footprint, energy consumption, and potential for utilizing eco-friendly refrigerants, contributing to sustainable and environmentally responsible cooling solutions.
- 4) *Integration of Renewable Energy*: Explore the integration of renewable energy sources, such as solar or waste heat recovery, to power or enhance the LiBr-water absorption refrigerant system. Investigate the feasibility and efficiency of coupling the system with renewable energy technologies for sustainable operation.
- 5) *Optimization under Varying Operating Conditions*: Extend the optimization studies to encompass a wider range of operating conditions, including variations in ambient temperature, humidity, and cooling load. This will provide a more comprehensive understanding of the system's performance across diverse scenarios.
- 6) *Multi-Objective Optimization*: Undertake multi-objective optimization studies to concurrently optimize multiple responses, such as COP, environmental impact, and system cost. This holistic approach can lead to more balanced and sustainable system designs.
- 7) *Machine Learning Applications*: Explore the application of machine learning techniques for predicting and optimizing the system's performance. Machine learning algorithms can analyze complex relationships within the system and offer insights for further improvements.
- 8) *Economic Feasibility Analysis*: Conduct an economic feasibility analysis to assess the cost-effectiveness of implementing the optimized LiBr-water absorption refrigerant system. Consider factors such as initial investment, operational costs, and potential return on investment.
- 9) *Scale-Up Studies*: Investigate the scalability of the optimized system for larger applications and explore the potential for commercialization. Scaling up the system would involve addressing challenges related to system dynamics, materials, and overall efficiency at an industrial scale.

#### Nomenclature

$T_g$	=	Generator Temperature (°C)
$T_a$	=	Absorber Temperature (°C)
$T_c$	=	Condenser Temperature (°C)
$T_e$	=	Evaporator Temperature (°C)
$\dot{m}$	=	Mass flow rate (kg/s)
$W_p$	=	Work input into the pump (kw)
$Q_a$	=	Heat rejected by the Absorber (kw)
$Q_g$	=	Heat input into the Generator (kw)
$Q_e$	=	Heat absorbed in the Evaporator (kw)
$Q_c$	=	Heat rejected in the Condenser (kw)
$y$	=	Dependent variable
$x$	=	Independent variable
$\beta$	=	Regression coefficient
$\varepsilon$	=	Experimental error

#### REFERENCES

- [1] Wang, Rui, Z. Z. Xu, Q.W. Pan, S. X. Du, and Zefeng Xia. 2016. "Solar Driven Air Conditioning and Refrigeration Systems Corresponding to Various Heating Source Temperatures." *Applied Energy* 169: 846–56. <https://doi.org/10.1016/j.apenergy.2016.02.049>.
- [2] Salhi, K., Mourad Korichi, and Khaled Mohamed Ramadan. 2018. "Thermodynamic and Thermo-Economic Analysis of Compression–Absorption Cascade Refrigeration System Using Low-GWP HFO Refrigerant Powered by Geothermal Energy." *International Journal of Refrigeration-Revue Internationale Du Froid* 94: 214–29. <https://doi.org/10.1016/j.jrefrig.2018.03.017>.
- [3] Marashli, Abdullah, Enas Alfanatseh, Mohammad Shalby, and Mohamed R. Gomaa. 2022. "Modelling Single-Effect of Lithium Bromide-Water (LiBr–H<sub>2</sub>O) Driven by an Evacuated Solar Tube Collector in Ma'an City (Jordan) Case Study." *Case Studies in Thermal Engineering* 37: 102239. <https://doi.org/10.1016/j.csite.2022.102239>.
- [4] Özakın, Ahmet Numan, and Ferhat Kaya. 2020. "Experimental Thermodynamic Analysis of Air-Based PVT System Using Fins in Different Materials: Optimization of Control Parameters by Taguchi Method and ANOVA." *Solar Energy* 197: 199–211. <https://doi.org/10.1016/j.solener.2019.12.077>.
- [5] Huirem, Boris, and P.K. Sahoo. 2020. "Thermodynamic Modeling and Performance Optimization of a Solar-Assisted Vapor Absorption Refrigeration System (SAVARS)." *International Journal of Air-Conditioning and Refrigeration* 28 (01): 2050006. <https://doi.org/10.1142/s2010132520500066>.
- [6] Agarwal, Shyam, Akhilesh Arora, and B.B. Arora. 2020. "Energy and Exergy Analysis of Vapor Compression–Triple Effect Absorption Cascade Refrigeration System." *Engineering Science and Technology, an International Journal* 23 (3): 625–41. <https://doi.org/10.1016/j.jestch.2019.08.001>.

- [7] Azhar, Md., and M. Altamush Siddiqui. 2020. "Comprehensive Exergy Analysis and Optimization of Operating Parameters for Double Effect Parallel Flow Absorption Refrigeration Cycle." *Thermal Science and Engineering Progress* 16: 100464. <https://doi.org/10.1016/j.tsep.2019.100464>.
- [8] Pandya, Bhargav, Nishant Modi, Ravi Upadhyai, and Jatin Patel. 2019. "Thermodynamic Performance and Comparison of Solar Assisted Double Effect Absorption Cooling System with LiCl-H<sub>2</sub>O and LiBr-H<sub>2</sub>O Working Fluid." *Building Simulation* 12 (6): 1063–75. <https://doi.org/10.1007/s12273-019-0535-3>.
- [9] Talpada, Jagdish S., and P.V. Ramana. 2018. "A Review on Performance Improvement of an Absorption Refrigeration System by Modification of Basic Cycle." *International Journal of Ambient Energy* 40 (6): 661–73. <https://doi.org/10.1080/01430750.2017.1423379>.
- [10] Iffa, Ridha Ben, Nahla Bouaziz, and Lakdar Kairouani. 2017. "Optimization of Absorption Refrigeration Systems by Design of Experiments Method." *Energy Procedia* 139: 280–87. <https://doi.org/10.1016/j.egypro.2017.11.209>.
- [11] Sivasakthivel, T., K. Murugesan, and Hywel Rhys Thomas. 2014. "Optimization of Operating Parameters of Ground Source Heat Pump System for Space Heating and Cooling by Taguchi Method and Utility Concept." *Applied Energy* 116: 76–85. <https://doi.org/10.1016/j.apenergy.2013.10.065>.
- [12] Karamangil, M. I., Salih Coskun, Omer Kaynakli, and Nurettin Yamankaradeniz. 2010. "A Simulation Study of Performance Evaluation of Single-Stage Absorption Refrigeration System Using Conventional Working Fluids and Alternatives." *Renewable and Sustainable Energy Reviews* 14 (7): 1969–78. <https://doi.org/10.1016/j.rser.2010.04.008>.
- [13] Patil, Prashant, Nitin Kardekar, and Dhanapal Kamble. 2023. "Performance Analysis and Optimization of Nano Particle Base LiBr-H<sub>2</sub>O Vapor Absorption System by Using Taguchi, Grey Relational Analysis and ANOVA." *Materials Today: Proceedings* 72: 1413–19. <https://doi.org/10.1016/j.matpr.2022.09.340>.
- [14] Darwish, Naif A., S. Al-Hashimi, and Ali Almansoori. 2008. "Performance Analysis and Evaluation of a Commercial Absorption-Refrigeration Water-Ammonia (ARWA) System." *International Journal of Refrigeration-Revue Internationale Du Froid* 31 (7): 1214–23. <https://doi.org/10.1016/j.ijrefrig.2008.02.005>.
- [15] Jadidi, H., Mansoor Keyanpour-Rad, Hamidreza Haghgou, B. Chodani, S. Kianpour Rad, and M. Hasheminejad. 2022. "Energy and Exergy Simulation Analysis and Comparative Study of Solar Ejector Cooling System Using TRNSYS for Two Climates of Iran." *Heliyon* 8 (8): e10144. <https://doi.org/10.1016/j.heliyon.2022.e10144>.
- [16] Montgomery, Douglas C., Raymond H. Myers, Walter H. Carter, and G. Geoffrey Vining. 2005. "The Hierarchy Principle in Designed Industrial Experiments." *Quality and Reliability Engineering International* 21 (2): 197–201. <https://doi.org/10.1002/qre.615>.
- [17] Solanki, Alka, and Yash Pal. 2022. "Evaluation and Optimization of Single-Effect Vapour Absorption System for the Dairy Industry Using Design of Experiment Approach." *Journal of Thermal Engineering* 8 (5): 619–31. <https://doi.org/10.18186/thermal.1189093>.
- [18] Kazemian, Mohammad, Gandjalikhan S. A. Nassab, and Ebrahim Jahanshahi Javaran. 2020. "Comparative Study of Box-Behnken and Central Composite Designs to Investigate the Effective Parameters of Ammonia-Water Absorption Refrigerant System." *Proceedings of the Institution of Mechanical Engineers, Part C: Journal of Mechanical Engineering Science* 235 (16): 3095–3108. <https://doi.org/10.1177/0954406220959097>.
- [19] Goyal, Ashwini, Ahmad Faizan Sherwani, and Deepak Tiwari. 2019. "Optimization of Cyclic Parameters for ORC System Using Response Surface Methodology (RSM)." *Energy Sources, Part A: Recovery, Utilization, and Environmental Effects* 43 (8): 993–1006. <https://doi.org/10.1080/15567036.2019.1633443>.
- [20] Gambhir, Deshdeep, Ahmad Faizan Sherwani, Akhilesh Arora, and Ashwini. 2022. "Parametric Optimization of Blowdown Operated Double-Effect Vapour Absorption Refrigeration System." *Journal of Thermal Engineering* 8 (1): 78–89. <https://doi.org/10.18186/thermal.1067035>.
- [21] Myers, Raymond H., André I. Khuri, and W. H. Carter. 1989. "Response Surface Methodology: 1966-1988." *Technometrics* 31 (2): 137. <https://doi.org/10.2307/1268813>.
- [22] Canbolat, Ahmet Serhan, Ali Husnu Bademlioglu, Nurullah Arslanoglu, and Ömer Kaynakli. 2019a. "Performance Optimization of Absorption Refrigeration Systems Using Taguchi, ANOVA and Grey Relational Analysis Methods." *Journal of Cleaner Production* 229: 874–85. <https://doi.org/10.1016/j.jclepro.2019.05.020>.
- [23] Ketfi, Omar, Mustapha Merzouk, Nachida Kasbadji Merzouk, and Said El Metenani. 2015. "Performance of a Single Effect Solar Absorption Cooling System (LiBr-H<sub>2</sub>O)." *Energy Procedia* 74: 130–38. <https://doi.org/10.1016/j.egypro.2015.07.534>.
- [24] Kaushik, S.C., and Akhilesh Arora. 2009. "Energy and Exergy Analysis of Single Effect and Series Flow Double Effect Water-Lithium Bromide Absorption Refrigeration Systems." *International Journal of Refrigeration-Revue Internationale Du Froid* 32 (6): 1247–58. <https://doi.org/10.1016/j.ijrefrig.2009.01.017>.
- [25] Modi, Bhaumik, Anurag Mudgal, and Bhavesh Patel. 2017. "Energy and Exergy Investigation of Small Capacity Single Effect Lithium Bromide Absorption Refrigeration System." *Energy Procedia* 109: 203–10. <https://doi.org/10.1016/j.egypro.2017.03.040>.





10.22214/IJRASET



45.98



IMPACT FACTOR:  
7.129



IMPACT FACTOR:  
7.429



# INTERNATIONAL JOURNAL FOR RESEARCH

IN APPLIED SCIENCE & ENGINEERING TECHNOLOGY

Call : 08813907089  (24\*7 Support on Whatsapp)